Investigation of Front Propagation in an Electrochemical System: Experiments and Numerical Simulations *

G. Flätgen, K. Krischer, and G. Ertl

Fritz-Haber-Institut der Max-Planck-Gesellschaft, Faradayweg 4–6, D-14195 Berlin, Germany

Z. Naturforsch. **50a**, 1097–1104 (1995); received August 16, 1995

We examined the spatio-temporal behavior of an electrochemical system in the bistable regime, in which the system might take on either a high current density state (active) or a low current density state (passive) at one value of the externally applied voltage. The transition from the passive to the active state is accompanied by accelerating fronts with sharp interfaces, whereas the reverse transition from the active to the passive state exhibits much smoother spatial variations. Also the evolution of the total current density displays qualitative differences in the two cases. Both, the differences of the spatial patterns as well as those of the total current densities are reproduced with a mathematical model, which also reveals the origin of the asymmetry of the transitions: a global coupling, intrinsic in all electrochemical systems, in combination with the specific dependence of the reaction current on the electrode potential.

I. Introduction

The connection between local and global behavior is an important aspect of pattern formation: On the one hand, the global behavior can often easily be observed, whereas it might require enormous efforts to visualize local structures [1]. If it is possible to draw conclusion on spatial patterns from a global quantity, much work can be saved. On the other hand, and even more importantly, the dynamics at any point might depend on the global state of the system; with other words, a change of the state at one point influences all parts of the electrode, no matter how far apart they are. Such a phenomenon is called global coupling and is currently an intense field of research [2–7].

The aim of this paper is to outline the connection between local and global quantities in electrochemical systems. Thereby we will touch both of the above mentioned points: We will discuss under which conditions it is possible to gain information about the velocity of a front in a bistable system from the total current density. Furthermore, the reaction rate at one point of the electrode is coupled to the reaction rates at every point at the electrode via the electrolyte. In this sense electrochemical systems possess an intrinsic global coupling.

These points will be demonstrated with experiments as well as simulations on a mechanistically well understood reaction [8, 9]: the reduction of peroxodisulphate ($S_2O_8^{2-}$) to sulphate (SO_4^{2-}) at Ag electrodes. This reaction displays bistable behavior in a certain parameter range. Transitions between the two stable states are mediated via fronts. These transitions are not symmetric but show different behavior in the two possible directions. Up to now we presented the results for the transitions from the passive (low current density) to the active (high current density) state [10, 11]. Guided by our measurements, we proposed a model that reproduces the characteristics of this transition [12]. In this paper we present data of the active/passive transition and point out the difference to the passive/active transition. A comparison of the experimental and numerical data reveals the origin of the asymmetry of the transitions. Furthermore, it becomes clear, under which conditions one has to be cautious when drawing conclusions from the global current on the local behavior.

II. Experiment and Model

The experimental setup and the derivation of the model are described in detail in [10] and [12], respectively. In this section we summarize only those points of the experiments and the model which are essential for the further understanding.

---

* Paper presented at the 5th Annual Meeting of ENGADYN, Grenoble, October 10–13, 1994.

Reprint requests to Dr. K. Krischer, email: Krischer@fhi-berlin.mpg.de, Fax: 8413 5106

0932-0784 / 95 / 1200-1097 $ 06.00 © – Verlag der Zeitschrift für Naturforschung, D-72027 Tübingen

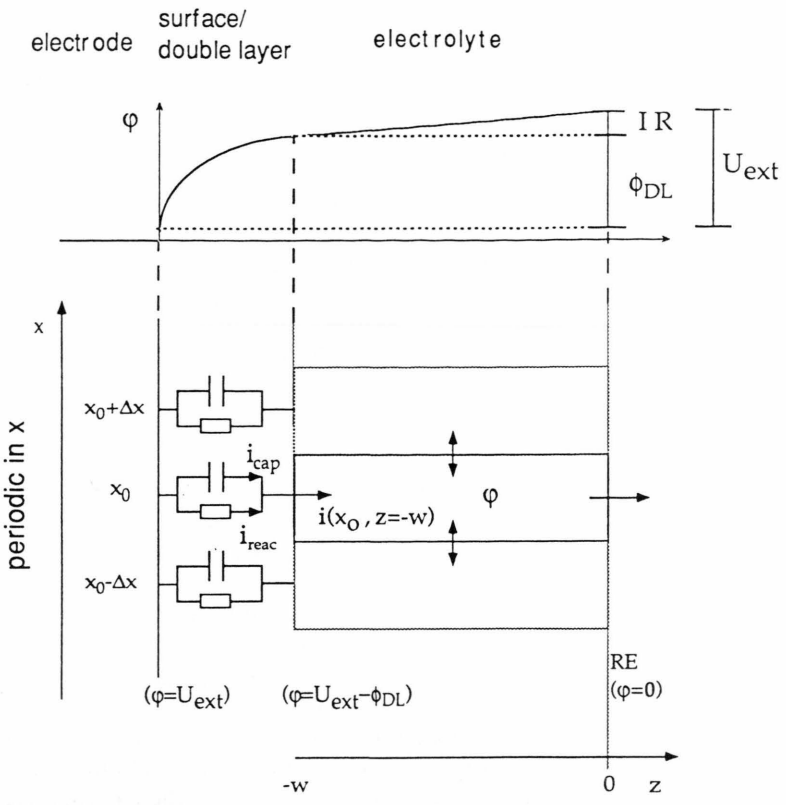

Fig. 1. Equivalent circuit for an electrochemical system (bottom) and potential profile between working electrode and equipotential surface (top). The external potential, U_{ext}, is composed of the potential drop across the double layer, ϕ_{DL}, (corresponding to the voltage drop across the capacitor in the equivalent circuit) and the Ohmic potential drop, IR, in the electrolyte.

An Ag ring is used as working electrode and immersed in the electrolyte consisting of $S_2O_8^{2-}$, SO_4^{2-}, H_2SO_4. At the interface electrode/electrolyte a space charge region the so-called double layer, develops. The potential drop across this double layer, ϕ_{DL}, can be changed by applying a constant voltage, U_{ext}, between the working electrode and a reference electrode, which is placed far away from the working electrode. At the applied voltages $S^2O_8^{2-}$ is reduced to SO_4^{2-}, leading to a current flow through the cell. The externally applied voltage U_{ext} is composed of the Ohmic potential drop between the working and reference electrode and the potential drop across the double layer, ϕ_{DL}. If there is an inhomogenous current density at the electrode (resulting from a spatial pattern of the potential drop, ϕ_{DL}), it will continue in the electrolyte and can be measured with a micro potential-probe close to the Ag-ring. We obtained a spatial resolution by rotating the Ag-ring over two stationary micro potential-probes.

Figure 1 displays the equivalent circuit of the experimental system: The electrode can be thought as a series of capacitors connected in parallel to non-Ohmic resistors. The capacitor describes the charging of the double layer. The potential dependence of the reaction current at the interface Ag/electrolyte is described by the nonlinear resistor. It displays a negative differential region which is necessary for pattern formation. The patterns consist of spatio-temporal variations of the potential drop ϕ_{DL}. These potential differences influence the potential in the electrolyte up to the equipotential plane at the place of the reference electrode ($z=0$).

A model has to describe the potential in the electrolyte and the temporal evolution of the potential drop at the interface. The potential in the electrolyte, φ, is determined by Laplace's equation

$$\Delta\varphi = 0 \tag{1}$$

with the following boundary conditions (b.c.):

$$i_{cap} = C\dot{\phi}_{DL} = -i_{reac} - \sigma \left.\frac{\partial\varphi}{\partial z}\right|_{z=-w}, \tag{2}$$

$$\varphi(x, z=0) \equiv 0 \quad \text{and}$$

$$U_{ext} - \phi_{DL}(x) = \varphi(x, z=-w), \tag{3}$$

$$\varphi(x, z) = \varphi(x+2\pi, z). \tag{4}$$

The first b.c., (2), describes the temporal evolution of the potential drop across the double layer ϕ_{DL} and follows from the current balance. i_{cap} denotes the charging current of the double layer, C the capacitance, and σ the conductivity of the solution. We assume that all concentrations are constant, and hence σ is a constant. Equation (3) results from the potentiostatic operation mode, and (4) desribes periodic b.c. parallel to the electrode.

From the continuity equation it follows that the migration current at the working electrode ($z=-w$) can be expressed by the difference of the migration currents parallel to the electrode and the current at the equipotential plane ($z=0$, Fig. 1)

$$\left.\frac{\partial\varphi}{\partial z}\right|_{z=-w} = \int_{-w}^{0} \frac{\partial^2\varphi}{\partial x^2}\,\mathrm{d}z + \left.\frac{\partial\varphi}{\partial z}\right|_{z=0}. \tag{5}$$

In this formulation it becomes apparent that the potential drop at the boundary is globally, or better non-locally, couples via the electrolyte.

III. Experimental Results

The reaction displays a bistable region in the current voltage characteristic (Figure 2). At a fixed value of the externally applied voltage, U_{ext}, there exist two stable current densities. As already mentioned, U_{ext} is composed of the voltage drop across the double layer, ϕ_{DL}, and the Ohmic potential drop, IR, in the electrolyte. Hence, the different current densities are connected with different voltage drops across the interface. We investigate the local behavior of the potential during a transition from one stable state to the other. At the higher voltage end of the bistability the active state is more stable than the passive one, and, hence, after a passive/active transition the system stays in the active state. At more negative potentials only active/passive transitions occur, and the system remains in the passive state.

In the following we compare both transitions: Consider first the passive/active transition. Figure 3a displays the time trace of the global current density during the transition. The corresponding local behavior can be seen in Fig. 3b, where the potential is plotted as a function of position and time. The amount of the total current increases continuously during the transition, and it is striking that the increase is faster than linearly. A comparison with Fig. 3b shows that the increase of the current starts when a small nucleus of

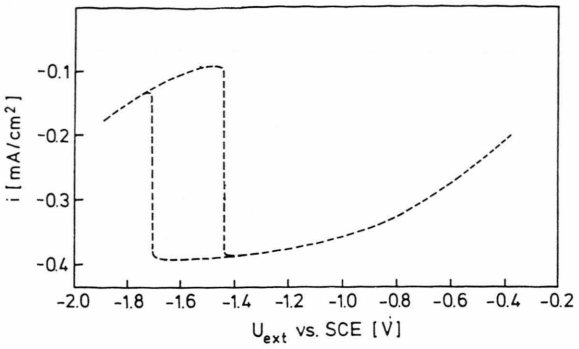

Fig. 2. Experiment current-voltage curve of a solution containing 1 mM $S_2O_8^{2-}$ and 0.5 mM SO_4^{2-}, rotation frequency $f=40$ Hz. The current displays bistable behavior.

the active state is formed, and while this nucleus spreads in both directions, the current increases further until the whole electrode is in the active state. From the space time plot it is evident that the velocity with which the active state expands, increases with time; this means that the motion of the interface is accelerated. In fact, this information is already contained in the global current density. Let us assume that during the transition a part of the electrode is in the active state and the rest of it in the passive state. In this case, the velocity of the front can be obtained from the differential change of the current I:

$$\begin{aligned}\mathrm{d}I &= i_a\,\mathrm{d}A_a + i_p\,\mathrm{d}A_p \\ &= i_a 2b(v_F\,\mathrm{d}t) + i_p 2b(-v_F\,\mathrm{d}t),\end{aligned} \tag{6}$$

where A_a is the area of the active state, A_p the area of the passive state, respectively. v_F is the front velocity, b is the width of the ring and $v_F\,\mathrm{d}t$ the differential change of the distance covered since the nucleation of the front. Figure 3c shows a comparison of the velocities calculated from the global current (dashed line) and the velocities resulting from the local measurements. With both methods the same velocities are obtained.

Let us now look at an active/passive transition: In Fig. 4 the total current (Fig. 4a) and the potential along the electrode (Fig. 4b) are shown as functions of time. As one would expect, the amount of the total current decreases monotonically during the transition, and by analogy to the passive-active transition one would guess that also here a nucleation center of the passive state is formed which expands over the whole electrode. The space time plot, however, shows a different behavior: Neither starts the transition at a

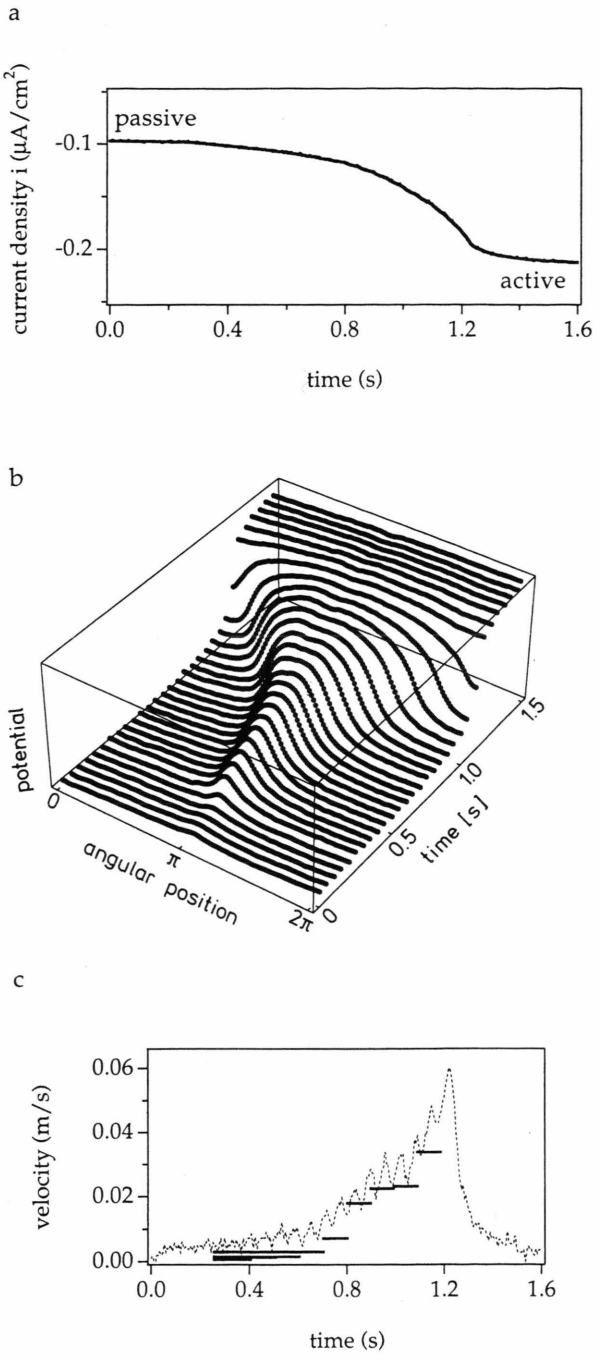

Fig. 3. Experimental global and local behavior of the passive/active transition (a) time series of the global current i, (b) spatio-temporal plot of the local potential, (c) front velocity versus time. The bars show the mean velocity obtained from the micro potential-probes. The dashed line displays the velocity obtained from the derivative of the total current, (6). Parameters: $U_{ext} = -1.36$ V, $f = 20$ Hz, $c_{S_2O_8^{2-}} = 0.1$ mM, $c_{SO_4^{2-}} = 0.1$ mM, pH 5, circumference of the electrode $L = 3.46$ cm.

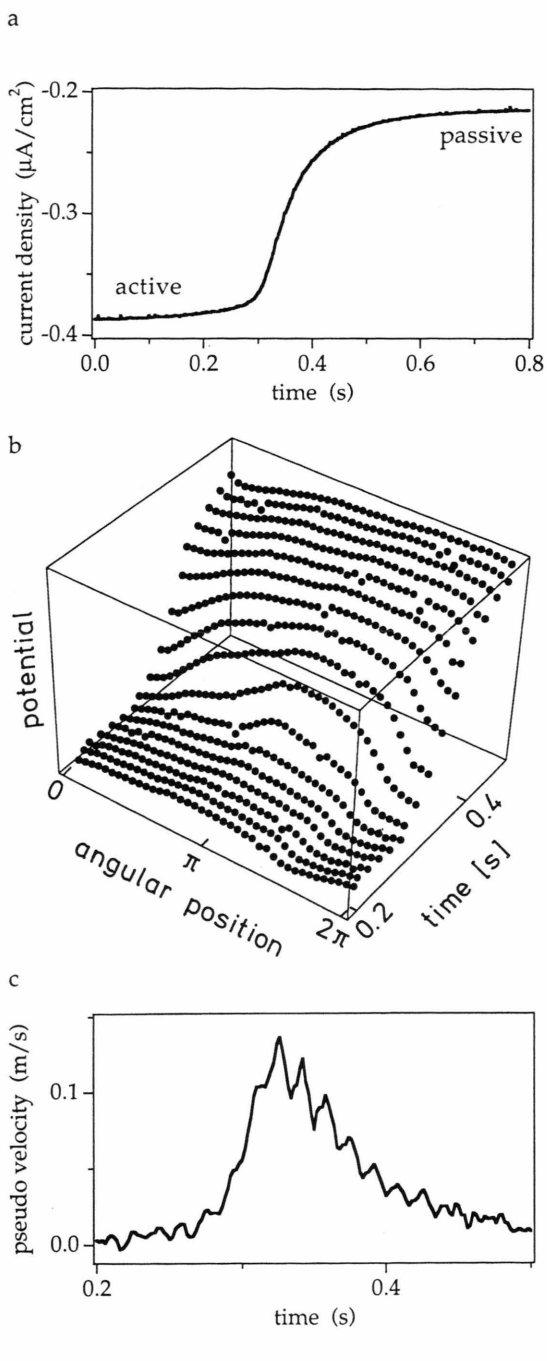

Fig. 4. Experimental global and local behavior of the active/passive transition (a) time series of the total current i, (b) spatio-temporal plot of the local potential, (c) 'pseudo front velocity' versus time as obtained from the total current, (6). Parameters: $U_{ext} = -1.36$ V, $f = 20$ Hz, $c_{S_2O_8^{2-}} = 0.1$ mM, $c_{SO_4^{2-}} = 0.1$ mM, pH 5, circumference of the electrode $L = 3.46$ cm.

distinct point on the electrode, nor is there a clear front spreading across the Ag-ring. Rather, in the beginning of the transition a broad, not well defined region acquires a higher potential. During the transition this region becomes larger, though less distinct, whereas the potential slowly changes all over the electrode. With other words, although there are some structures present, no moving interface or front can be defined. Under different experimental conditions, the transition exhibits front-like behavior; however, the interface of an active/passive front is always broader than the one of a passive/active one. Also the temporal derivative of the total current exhibits qualitative differences (Figure 4c). It does not monotonically increase with time, but a sharp rise of this 'pseudo velocity' is followed by a longer period with decreasing velocity. This feature is always found during the active/passive transition, independent of how localized the front is. Before we discuss the differences of the transitions, corresponding numerical simulations shall be presented.

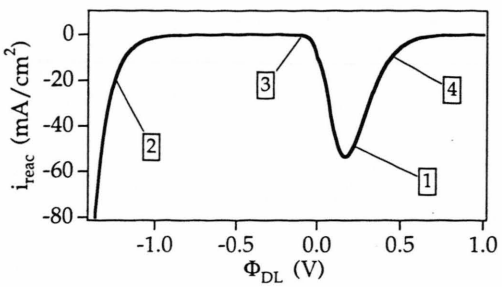

Fig. 5. Reaction current, i_{reac}, versus potential drop, ϕ_{DL}, for a solution containing 0.1 mM $S_2O_8^{2-}$ and 5 mM SO_4^{2-}. The start and end values of the simulated transitions (equal to the steady states of the homogeneous system) are indicated by numbers: 1 and 2 for the active/passive, 3 and 4 for the passive/active transition.

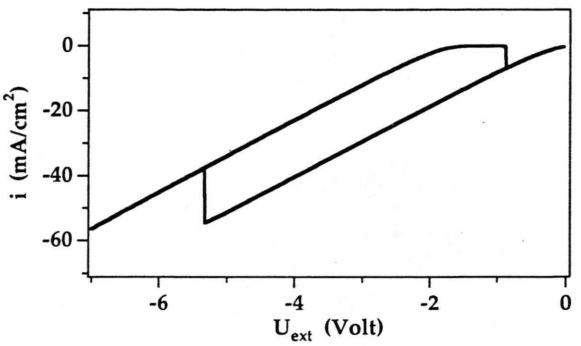

Fig. 6. Simulated current voltage characteristic with the reaction current from Figure 5.

IV. Numerical Results

In order to solve (1)–(4), the reaction current, i_{reac}, has to be specified. It was shown that the reduction of $S_2O_8^{2-}$ obeys a Butler-Volmer kinetics with Frumkin correction [8, 9], and we used the expression and the constants given in [9, 12]. The corresponding current-voltage dependence is shown in Figure 5. Laplace's equation was solved by a series expansion, and the simulation of the temporal evolution of ϕ_{DL} was performed explicitly or with some integration solver.

As can be seen in Fig. 6, the simulated global current density displays bistable behavior. Spatiotemporal plots of passive/active and active/passive transitions are shown in Figs. 7 and 8. For both simulations the parameters were fixed close to the respective saddle-node bifurcations (which mark the end of the bistable behavior), and the electrode was set in one steady state with a small perturbation in the other steady state. In the case of the passive/active transition, the initial nucleus spreads over the whole electrode in a front like behavior (Figure 7b). The velocity of the front increases with time, which can be better seen in Fig. 7c, where the temporal evolution of the velocity (obtained from the derivative of the global current (Fig. 8a)) is plotted. In contrast, during the active/passive transition (Fig. 8) the initial perturbation smears out without forming a localized, moving interface. Rather, already in the beginning of the transition every point of the electrode shows a marked temporal evolution, though the further away from the perturbance the point is, the smaller this evolution. As a result, the end of the transition is characterized by a nearly homogeneous relaxation to the passive steady state. These are exactly the characteristics that were observed experimentally under the same conditions. As a comparison of the calculated and measured derivative of the global current shows, even the triangular shape of this curve is reproduced in the calculations (Figure 8c). When changing the conditions (e.g., the concentrations), the simulations predict more front like solutions. The interface of the fronts remains, however, always flatter than during the passive/active transition.

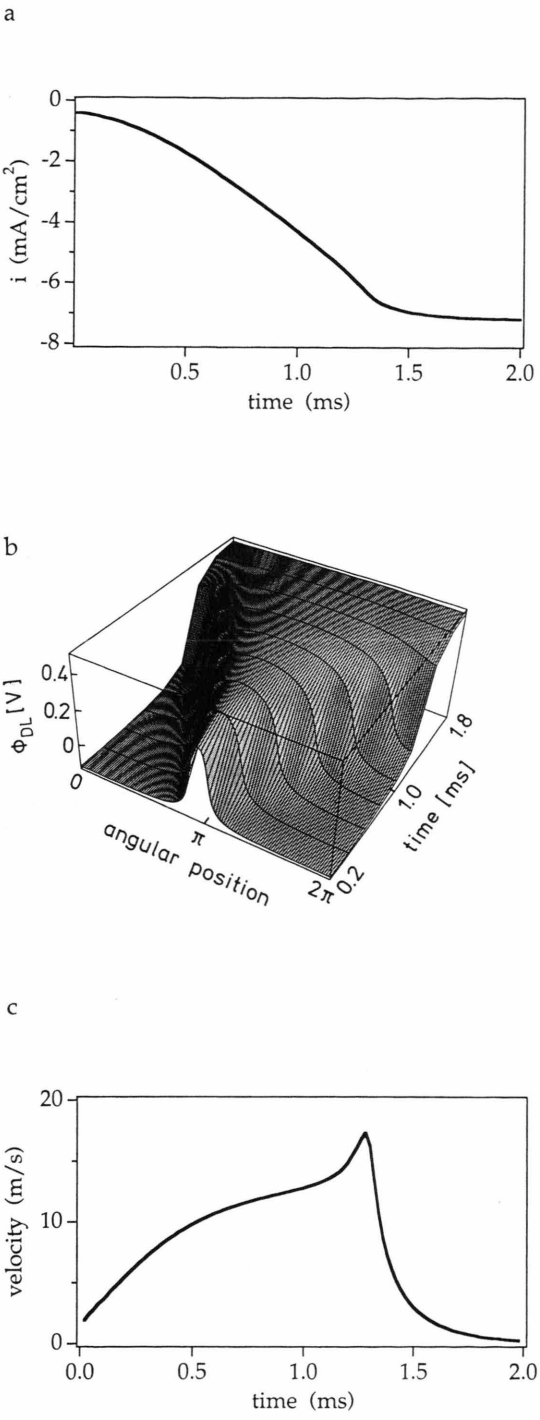

Fig. 7. Simulated global and local behavior of the passive/active transition (a) time series of the global current i, (b) spatio-temporal plot of the local potential, (c) velocity (obtained from the global current) versus time. Parameters: $U_{ext} = -0.9$ V, $c_{S_2O_8^{2-}} = 0.1$ mM, $c_{SO_4^{2-}} = 5$ mM, circumference of the electrode $L = 3$ cm.

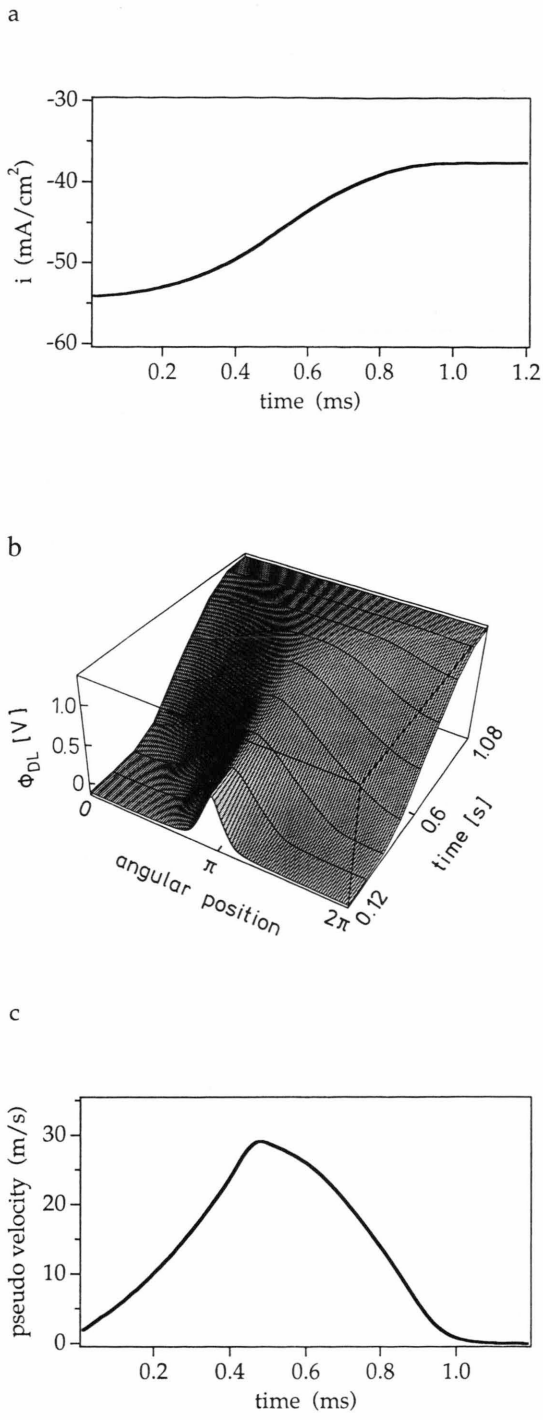

Fig. 8. Simulated global and local behavior of the active/passive transition (a) time series of the total current i, (b) spatio-temporal plot of the local potential, (c) 'pseudo velocity' (obtained from the global current) versus time. Parameters: $U_{ext} = -5.538$ V, $c_{S_2O_8^{2-}} = 0.1$ mM, $c_{SO_4^{2-}} = 5$ mM, pH 5, circumference of the electrode $L = 3$ cm.

V. Discussion

So far we have shown that the global and local behavior of the passive/active and active/passive transitions exhibited different behavior. During the passive/active transition front-like behavior was observed, and these fronts moved with increasing velocity. A direct measurement of the velocity agreed well with the calculation of it from the derivative of the global current. By contrast, much flatter interfaces were observed during the active/passive transition, up to situations where no sharp interfaces at all could be distinguished; rather the potential varied smoothly over the entire electrode. In addition, the derivative of the total current did not monotonically increase, but exhibited a maximum. All these features could be reproduced in the simulations.

The different spatial behavior as well as the different behavior of the global current density can be explained with the specific dependence of the current density, i_{reac}, on the potential drop across the double layer, ϕ_{DL} (see Figure 5). The numbers 1 and 2 in Fig. 5 mark the initial and end points of the active/passive, and the numbers 3 and 4 those of the passive/active transition. Obviously, the potential difference between the two steady states in the active/passive case is much larger than in the reverse case. The distance of the potential of the two states $|\phi_{\mathrm{DL,p}} - \phi_{\mathrm{DL,a}}|$ enters (2) in the term which contains the first spatial derivative of the potential, and therefore this term has a larger influence in the active/passive transition than in the passive/active one. This term represents a global coupling as via Laplace's equation and the boundary condition, the first derivative, depends on the potential distribution of the whole electrode, (5). In [12] we have shown that this global coupling leads to accelerating fronts of the passive/active transition. During the active/passive transition the global coupling is even more pronounced, which results in a negative 'shift' of the potential even far away from a passive region, giving rise to a flatter interface and, hence, to a more homogeneous transition. Note that a small shift of the potential at points which are far away from the interface also occurs in the passive/active transition.

We mentioned that for some experimental conditions front-like behavior was also observed during the active/passive transition. Whenever a moving interface could be defined, the motion of it was accelerated. However, never could one draw a conclusion from the total current on this acceleration as it was the case in the passive/active transition. This decrepancy can again be explained by the specific dependency of the reaction current on the potential (Figure 5). As already said, the global coupling causes a shift of the potential during the transition at every place of the electrode. Consider the effect of the shifts on the global current density: During the active/passive transition the part which is more in the active state and the part which is more in the passive state shift to more negative potential values at which the reaction rate is higher. This increase of the current upon a small shift of the potential is very pronounced for the passive state (point 4 in Figure 5). As a consequence, the decrease of the global current during the active/passive transition becomes smaller towards the end of the transition, which leads to the observed complex form of the global current shown in Fig. 4a for the experimental and in Fig. 8a for the simulated data, and the acceleration of the fronts does not show up in the total current. During the passive/active transition the parts shift towards more positive potentials. This means that the current density of the passive part shifts to higher currents while the one of the active part shifts towards lower current values. Hence, the effects of the shifts of the two states on the total current compensate each other. This fact keeps the error small when estimating the front velocity from the total current. Of course, such an estimation requires, in addition, that the shifts of the states themselves are small.

VI. Conclusion

In summary, a characteristic feature of electrochemical systems is that the electric field transmits information about a change of the local potential to every place at the electrode, i.e., electrochemical systems possess an intrinsic global coupling. Depending on the strength of this coupling and on the specific reaction current, the spatial structures may be localized or smeared out over a large region. Whether conclusion can be drawn from the total current on local quantities (e.g., the front velocity) has to be tested in each case separately. If the dependence of the reaction current on the potential drop across the double layer is known, it should be possible to answer this question with numerical simulations of (1)–(4). In the presented case, these equations reproduced even the subtleties of the experimental data.

Acknowledgements

It was a great pleasure to present these results at the ENGADYN Workshop in Grenoble and to discuss them with the participants.

[1] R. Richter, A. Kitel, G. Heinz, G. Flätgen, J. Peinke, and J. Parisi, Phys. Rev. B **49,** 8738 (1994).
[2] L. Schimansky-Geier, C. Zülicke, and E. Schöll, Physica A **188,** 436 (1992).
[3] F. Mertens, R. Imbihl, and A. Mikhailov, J. Chem. Phys. **99,** 8668 (1993).
[4] M. Bode, A. Reuter, R. Schmeling, and H.-G. Purwins, Physics Letters A **185,** 70 (1994).
[5] U. Middya and D. Luss, J. Chem. Phys. **100,** 3568 (1994).
[6] K. Krischer and A. Mikhailov, Phys. Rev. Lett. **73,** 3165 (1994).
[7] T. Christen, submitted.
[8] A. Frumkin, Z. Elektrochem. **59,** 807 (1955).
[9] W. Wolf, J. Ye, M. Purgand, M. Eiswirth, and K. Doblhofer, Ber. Bunsenges. Phys. Chem. **96,** 1797 (1992).
[10] G. Flätgen and K. Krischer, Phys. Rev. E, in press (1995).
[11] G. Flätgen, K. Krischer, B. Pettinger, K. Doblhofer, and G. Ertl, submitted.
[12] G. Flätgen, K. Krischer, and G. Ertl, submitted.